nature geoscience

LETTERS

PUBLISHED ONLINE: 13 APRIL 2015 | DOI: 10.1038/NGEO2412

Transient liquid water and water activity at Gale crater on Mars

F. Javier Martín-Torres[1,2*], María-Paz Zorzano[3], Patricia Valentín-Serrano[1,3], Ari-Matti Harri[4], Maria Genzer[4], Osku Kemppinen[4], Edgard G. Rivera-Valentin[5], Insoo Jun[6], James Wray[7], Morten Bo Madsen[8], Walter Goetz[9], Alfred S. McEwen[10], Craig Hardgrove[11], Nilton Renno[12], Vincent F. Chevrier[13], Michael Mischna[6], Rafael Navarro-González[14], Jesús Martínez-Frías[15], Pamela Conrad[16], Tim McConnochie[17], Charles Cockell[18], Gilles Berger[19], Ashwin R. Vasavada[6], Dawn Sumner[20] and David Vaniman[21]

Water is a requirement for life as we know it[1]. Indirect evidence of transient liquid water has been observed from orbiter on equatorial Mars[2], in contrast with expectations from large-scale climate models. The presence of perchlorate salts, which have been detected at Gale crater on equatorial Mars by the Curiosity rover[3,4], lowers the freezing temperature of water[5]. Moreover, perchlorates can form stable hydrated compounds and liquid solutions by absorbing atmospheric water vapour through deliquescence[6,7]. Here we analyse relative humidity, air temperature and ground temperature data from the Curiosity rover at Gale crater and find that the observations support the formation of night-time transient liquid brines in the uppermost 5 cm of the subsurface that then evaporate after sunrise. We also find that changes in the hydration state of salts within the uppermost 15 cm of the subsurface, as measured by Curiosity, are consistent with an active exchange of water at the atmosphere–soil interface. However, the water activity and temperature are probably too low to support terrestrial organisms[8]. Perchlorates are widespread on the surface of Mars[9] and we expect that liquid brines are abundant beyond equatorial regions where atmospheric humidity is higher and temperatures are lower.

At the appropriate range of relative humidity and temperature, perchlorates (ClO_4^-) deliquesce into the aqueous phase creating brines (that is, solutions of salt in water) that are stable in the liquid state. Deliquescence[6,7] occurs when, simultaneously, the ambient relative humidity (RH) is above the deliquescent relative humidity (DRH) of the deliquescent salt and the ambient temperature (T) is above the eutectic temperature (T_e) of the resulting solution. The stability of transient aqueous salt solutions on Mars was first postulated in the 1960s[10], and has been inferred from indirect observations at polar and near-polar regions[7,11]. The present-day activity of equatorial recurring slope lineae has been attributed to seasonal flow of brines[2] (Supplementary Fig. 1). Nevertheless, on the basis of the large-scale predictions of global circulation models (GCMs) and the remote-sensing large-scale observation of RH and T, it is believed that deliquescence conditions could be theoretically reached on the surface of Mars only poleward of ±60° and only during the northern spring[11,12] (when the water vapour content of the martian atmosphere peaks[13]). Transiently stable liquid water in the form of brines was unexpected at an equatorial region[11] such as Gale (4.6° S, 137.4° E, at 4.5 km below the datum), where the Mars Science Laboratory (MSL) landed and has been operating since 6 August 2012.

However, here we show that the RH, air temperature (T_a) and ground temperature (T_g) observations at Gale by the Rover Environmental Monitoring Station[14] (REMS) on the Curiosity rover at the MSL mission[15] are compatible with the presence of liquid brines during night time due to the increased RH associated with night-time lower ambient temperatures. Figure 1a shows the diurnal variation of the ground relative humidity and temperature (RH_g and T_g) for the sols (Martian days) corresponding to the beginning of each season: Ls = 90 (winter), 180 (spring), 270 (summer) and 360 (autumn). When one full martian year is analysed and compared with the phase diagram of Ca-perchlorate, the diurnal variation crosses at night time the boundary of liquid stability (REMS corresponding measurement data set shown in cyan) allowing for transient liquid stability at the ground surface (see Fig. 1b, and the diurnal cycle in Supplementary Figs 2 and 3). As shown in Supplementary Fig. 4, the local diurnal cycle also allows for transient liquid water stability in the uppermost 5 cm of the subsurface at night time during the full winter season. These conditions allowing for transient liquid water are not compatible with the known requirements for replication and metabolism of terrestrial microorganisms[8]; see Fig. 1b, where the phase diagram of Ca-perchlorate[6] is compared with the evolution of the (night time) minimum T_g and maximum RH_g (expressed as water activity (a.w.), which in equilibrium with the atmosphere is equal to the RH divided by 100). The diurnal maximum and minimum ground surface temperatures (T_g^{max} and T_g^{min}) measured by REMS throughout the mission and the diurnal range of modelled subsurface temperatures at a depth of 15 cm (T_{-15cm}) are shown in Fig. 2a. A fully coupled heat and mass transfer model assuming a constant thermal inertia has been used to estimate the diurnal subsurface temperature profile and water activity[16], based on REMS data. In parallel, a simplified subsurface model has been used to derive the mean diurnal T_{-15cm} (as extrapolation of the measured diurnal ground surface temperatures) accounting for the site-to-site variation of thermal inertia. At a depth of 15 cm and throughout all of the year and at all of the sites visited by Curiosity, the subsurface temperature (T_{-15cm}) is below the known temperature requirements for replication and metabolism of terrestrial microbial life forms (Fig. 2a).

Although the Phoenix lander provided data for late spring and early to mid summer[17,18], REMS measured for the first time the RH

A full list of author affiliations appears at the end of the paper.

© 2015 Macmillan Publishers Limited. All rights reserved

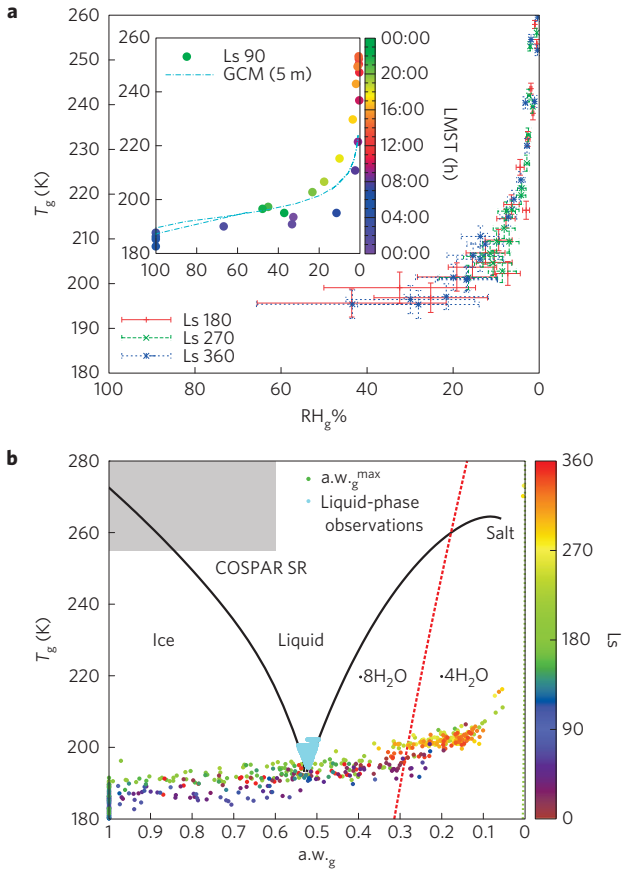

Figure 1 | Ground relative humidity, water activity and temperature at Gale crater and aqueous $Ca(ClO_4)_2$ stability conditions. a, Measured diurnal variation of RH_g and T_g at Ls = 90 (inset, LMST is indicated in colour scale), compared with a GCM simulation at 5 m (cyan curves in inset), and Ls = 180, 270 and 360 measurements. Error bars indicate either instrument error or derived magnitude error (see Supplementary Information). **b**, Phase diagram of Ca-perchlorate indicating the conditions where liquid brines, ·8H_2O, ·4H_2O and dehydrated (close to a.w. = 0 axis) states are formed. Annual measured variation of daily a.w.$_g^{max}$ (and T_g^{min}; Ls is indicated in colour coding) and measured environmental conditions that match stability liquid conditions (dots in cyan) are shown. The dotted red line indicates the transition between different hydration states.

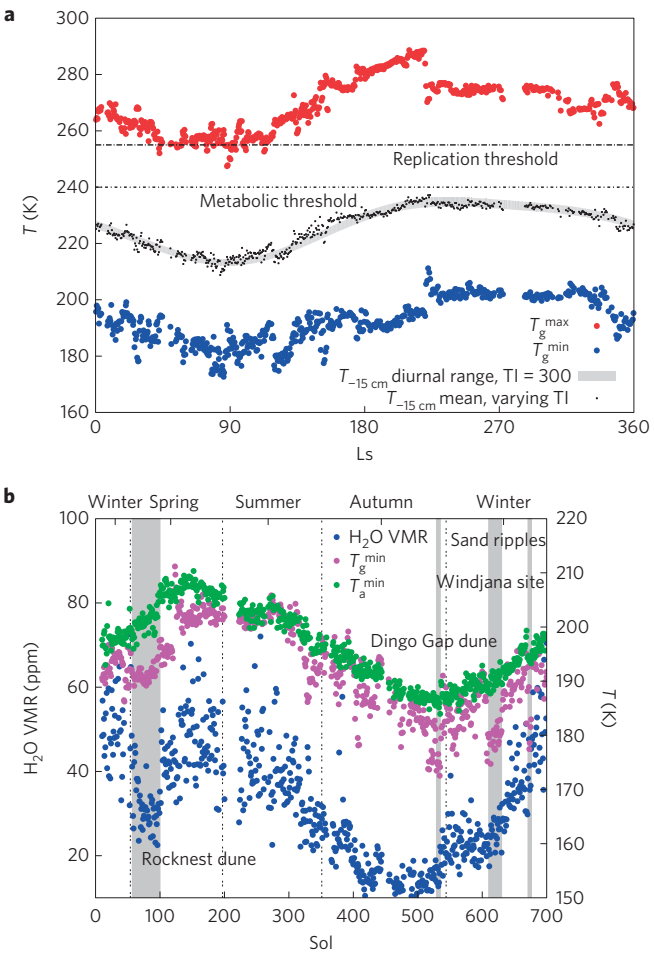

Figure 2 | Surface and subsurface temperatures, night-time H_2O VMR and air temperature. a, During a few hours every day, the surface is above the thermal threshold for microbial replication; however, at these hours the RH_g (and a.w.$_g$) is 0. $T_{-15\,cm}$ is so low that it goes below the threshold of replication and even of metabolism of known terrestrial microorganisms[8]. TI, thermal inertia. **b**, The sudden increase in H_2O VMR as the rover leaves the sand areas, shaded in grey, is consistent with the existence of a local exchange of H_2O between the soil and atmosphere. Dashed lines indicate the transition between seasons.

near the surface (1.6 m above the surface) for a full martian year, providing for the first time *in situ* characterization of the full diurnal (Supplementary Fig. 2 and Fig. 1a) and seasonal (Figs 1b and 2b and Supplementary Fig. 5) cycles of water on the martian surface[19]. The Curiosity rover of the MSL mission landed at 15:03 local mean solar time (LMST) on Mars (6 August 2012, 05:18 UTC spacecraft event time), at the end of the local winter (Ls = 150.7), and after 2 Earth years of operation a new winter season has started at Gale. Figure 1a shows a repetitive diurnal cadence in RH and T, and Supplementary Fig. 5 shows its evolution through seasons. It is in agreement with past mission models[11] and with the profile expected by GCM simulations for the lowest boundary-layer height of the models (at 5 m; ref. 20; see Fig. 1a inset). On a seasonal scale, these curves vary according to the planetary circulation of atmospheric water vapour with minimum RH in summer and maxima in winter (Supplementary Fig. 5). The sudden local water volume mixing ratio (VMR) decrement when the rover crosses a sand-covered area indicates a variation in the amount of water in the near surface that depends on the properties of the soil (see Fig. 2b).

Below 15 cm, the subsurface conditions are compatible with the existence of permanently hydrated perchlorates (Fig. 3a), which, owing to the low mean temperatures and the small diurnal and seasonal variations, are stable throughout the day and during all of the seasons at Gale crater. An analysis of the time stamp (in LMST and Ls) of the coexisting (T, RH) conditions that match the liquid state of Ca-perchlorate, at the surface (0 cm) and at 5 cm below the surface (−5 cm) respectively, indicates that liquid Ca-perchlorate brines are stable in the uppermost 5 cm during winter from sunset to sunrise and during the rest of the year for shorter windows of time, showing the expected Ls-time dependences (Fig. 3b). The upper layers of the regolith show such a large diurnal and seasonal thermal variation (and correspondingly a large RH variation) that the a.w. and T conditions cross several boundaries of Ca-perchlorate hydration states allowing for an active soil–atmosphere water exchange process on diurnal and seasonal timescales. Supplementary Fig. 6 shows that the daytime conditions are so dry at the uppermost centimetre of the subsurface that perchlorates and other salts or hydrated phases within these depths shall lose the water absorbed at night time. We therefore expect the upper layer of the ground to be drier in the daytime than the perennially hydrated lower layer.

Measurements from the Dynamic Albedo of Neutrons[21] (DAN), an independent instrument on Curiosity, are consistent with a local

© 2015 Macmillan Publishers Limited. All rights reserved

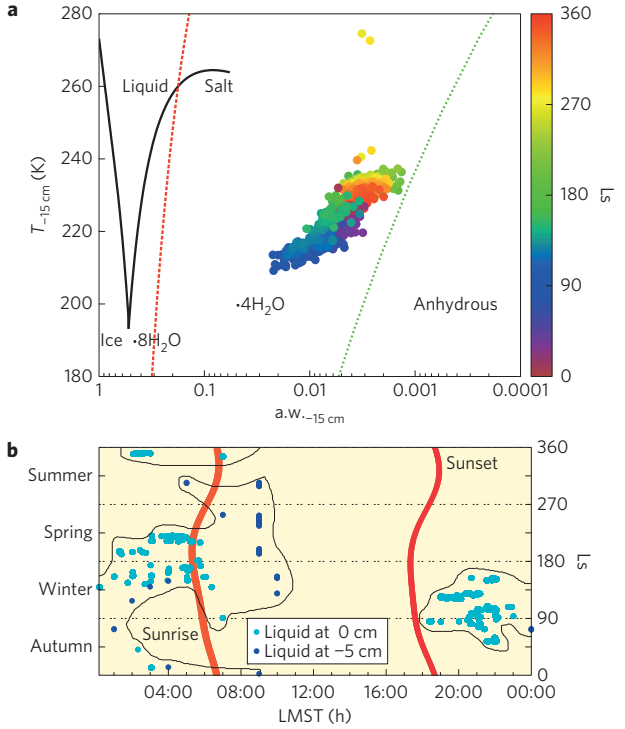

Figure 3 | Perennial hydration of subsurface Ca-perchlorate as ·4H_2O (and ·5H_2O for Mg-perchlorate, not shown), and moments of liquid surface stability. a, Diurnally averaged mean a.w.$_{-15\,cm}$ (assuming equilibrium) and $T_{-15\,cm}$ during the first martian year of the MSL mission superimposed on the phase diagram of Ca-perchlorate. Red and green dotted lines indicate the transition between different hydration states. **b**, Ls and LMST intervals when the surface environmental conditions permit the existence of Ca-perchlorate brines within the uppermost 5 cm of the subsurface. The points are (RH, T) values matching the conditions for the formation of liquid Ca-perchlorate at the ground and −5 cm. The sunrise and sunset times are included in red. The black line frames the period of time when liquid water is transiently stable.

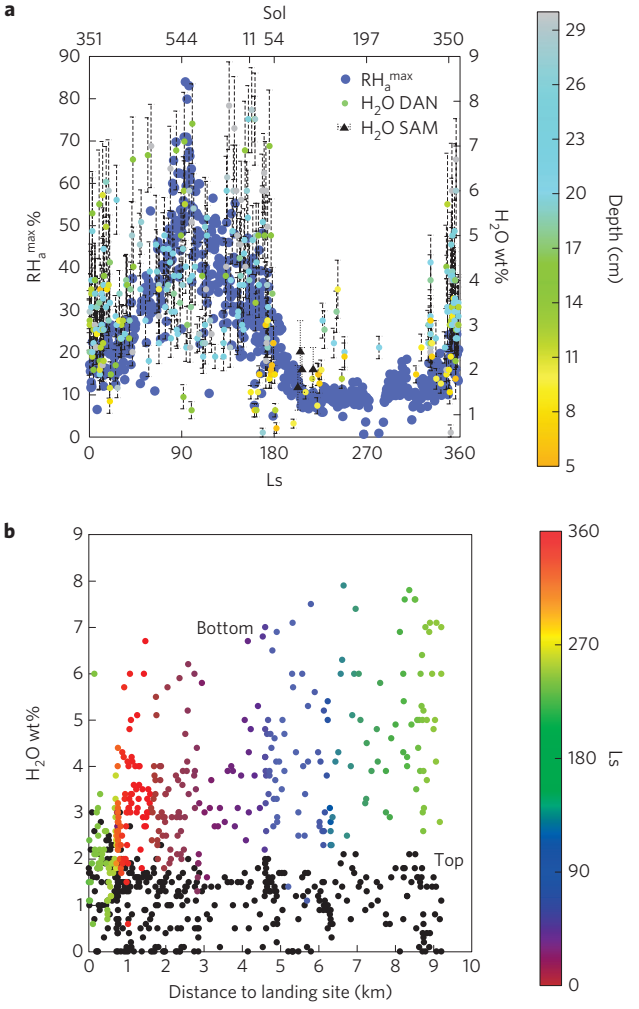

Figure 4 | Bottom-layer water content in correlation with the RH^{max}% and top-layer daytime dryness. a, DAN and Sample Analysis at Mars (SAM) H_2O wt% retrievals from daytime active measurements of subsurface bottom-layer water wt% and corresponding cutoff depth between the top drier layer and wetter bottom layer (indicated in colour coding). The correlation REMS/RH$_a^{max}$ suggests an equatorial seasonal cycle of hydration/dehydration of the subsurface materials caused by the interchange of water between atmosphere and regolith. Error bars indicate retrieval uncertainty (ref. 22). **b**, DAN-derived H_2O wt% for the bottom layer (colour coding indicates Ls) and corresponding drier upper-layer values (in black) as a function of Curiosity traverse.

active water cycle affecting soil moisture and a stratification of the hydration levels in the shallow subsurface: DAN has detected a significant level of subsurface water equivalent hydrogen whose wt% is correlated with the atmosphere RH% observations of REMS (Fig. 4a); and the results from the first year of DAN active measurements show that a best fit of the data is a two-layer regolith model, with a drier upper layer several centimetres deep with a wetter layer beneath[22] (Fig. 4b). REMS has also observed lower night-time atmospheric water vapour content over sand suggesting an enhanced local atmosphere–soil water cycle within sandy soil (Fig. 2b). H_2O molecules can also be bound to hydroxyl functional groups such as Si–OH and Al–OH–Al, and in these phases the wt% absorbed also increases with RH% (ref. 23).

Hydrated salts can be stable at conditions prevailing in the subsurface allowing water to be retained by the regolith throughout the diurnal cycle[24]. Beyond a certain depth (−15 cm) the subsurface temperature has negligible diurnal and seasonal variation, and the corresponding RH$_{<-15\,cm}$ is also stable and never reaches zero, allowing for the permanent stability of subsurface perchlorate or other salt hydrates[24], which only dehydrate at RH very close to 0. Daytime DAN measurements of the subsurface hydration vary with season (maximizing in the early winter) rather than with rover location at Gale crater (Fig. 4a,b) and the average depth of the transition from dry to wet layer is 17.1 cm ± 0.5 cm, which is at the depth where REMS observations combined with subsurface models predict the permanent hydration of salts. The subsurface water content (in the uppermost 60 cm) estimated from DAN measurements along the rover traverse is consistent with the existence of water bound to perchlorates (see Supplementary Fig. 7), which suggests that the widespread distribution of subsurface Cl signal, if in the form of perchlorates, may account for 1.2 wt% of the water signal as perennially stable perchlorate hydrates. The plausible perennially hydrated subsurface perchlorates may have implications for the analysis of the Cl wt% and H_2O wt% correlation measured from the Gamma Ray Spectrometer on board the Mars Odyssey[25]. The comparison of DAN and REMS data indicates that the subsurface water content and depth shows correlation with the diurnal temperature variation of the ground explored and is consistent with the stability depth of perchlorate hydrates (Supplementary Fig. 8).

Deliquescence provides a mechanism for the formation of thin films of liquid brines where large amounts of liquid are not available, with possible dissolution and precipitation of salts. Other possible pieces of evidence for this on Mars are: the Spirit rover finding

© 2015 Macmillan Publishers Limited. All rights reserved

of soluble ferric sulphates concentrated in a shallow subsurface soil layer, where they were apparently transported by a downward-migrating fluid[26]; the Opportunity rover finding of higher Cl concentrations in deeper strata relative to the modern Meridiani plains surface[27]; and the non-detection of hydrous salts in recurring slope lineae streaks[28]. Such brines could potentially mobilize other water-soluble salts from the surface to the subsurface leading to a vertical stratification of nitrates. The possible presence of nitrates in Gale crater has been inferred from the release of nitric oxide by the Sample Analysis at Mars instrument on Curiosity[29].

This detection at the equator (the driest and warmest region of the planet) of environmental conditions that can allow for transiently stable liquid brines defines a threshold condition for their presence. As perchlorates are widely distributed on the surface of Mars, this discovery implies that the rest of the planet should possess even more abundant brines owing to the expected greater atmospheric water content and lower temperatures. These findings have implications for Planetary Protection policies for future landed spacecraft[8]. Cl-bearing brines are very corrosive[30] and this may have implications on spacecraft design and surface operation (see Supplementary Fig. 9).

Methods

All of the Curiosity data that we have used are available at the NASA (National Aeronautics and Space Administration) Planetary Data System (http://atmos.nmsu.edu/PDS/data).

REMS measures three relevant variables: the air relative humidity (RH_a) and the air temperature (T_a), both at 1.6 m above the surface, and the ground surface (at 0 m) temperature (T_g). For a given acquisition, the corresponding ground surface relative humidity (RH_g), that is, relative humidity at 0 m, is calculated from T_a and T_g using the standard assumption that the H_2O measured at 1.6 m is the same as at the surface (that is, uniform mixing). Thus, any reported ground surface value is directly measured/calculated from REMS observations.

The diurnal subsurface temperature profile and water activity have been calculated using a fully coupled heat and mass transfer model assuming a constant thermal inertia, and using REMS measurements at the surface (0 m) and 1.6 m as inputs to the model. For simplicity, the subsurface data are modelled with only one data point per hour of acquisition (instead of the full data set of REMS measurements and ignoring the extended acquisitions). In parallel, a simplified subsurface model has been used to derive the mean diurnal temperature at −15 cm (as extrapolation of the measured diurnal ground surface temperatures) accounting for the site-to-site variation of thermal inertia. The heat and mass transfer model computes the subsurface profile and its diurnal evolution, and it is solved in such a way that the boundary condition at the surface is compliant with REMS measurements. It models the corresponding time evolution of RH_z at the subsurface depth z, and, in particular, it provides information about the environmental values at $z=-5$ cm and $z=-15$ cm of RH_{-5cm} and RH_{-15cm} as well as the corresponding (that is, time-correlated) temperature T_{-5cm} or T_{-15cm}. When the RH values are superimposed on the phase diagram of Ca-perchlorate, it is represented as water activity a.w. = RH/100.

Throughout the article, when pairs of T versus RH (or a.w. or H_2O VMR) data are plotted they are time correlated; that is, these two physical quantities coexist in time and are either directly measured by REMS, calculated in a straightforward manner (RH_g for the surface through the measured T_g, T_a and RH_a), or modelled (for the subsurface at a depth z) using REMS data as explained above. The measured maximum RH and a.w. values are reached when the measured temperature is minimal, so when these values are shown they are coexisting pairs. Mean or averaged values are daily means of the diurnal hourly measurements or of the diurnal hourly modelled values.

Detection of liquid-state points. All of the measured REMS data, over one full Martian year, have been screened for simultaneous pairs of (RH_g, T_g) that fall within the area of liquid-state stability of Ca-perchlorate (see Supplementary Fig. 4). When the environmental conditions (RH_g, T_g) were such that liquid conditions are plausible, the time stamp and the pair of corresponding values were stored. The values found through this liquid-phase screening are presented in Fig. 1b and Supplementary Fig. 4 (in cyan) and the time stamp in Fig. 3b. The liquid stability conditions are not maintained throughout the day; thus, we refer to 'transient' stability to account for the temporal character of this stability. A similar procedure is applied to the subsurface-modelled T_z and RH_z.

Subsurface thermal/a.w. model. Subsurface temperatures are calculated by solving the one-dimensional thermal diffusion equation using a forward Euler finite-element procedure with an element size of 0.05 cm and a time step of 100 s. The lower boundary condition includes a modest geothermal heat flux of 0.03 W m^{-2}. The surface boundary condition is radiative and includes the direct illumination, along with scattering and thermal emission. Temperature diffusion is modelled to a depth of 4 m, which is well below the annual skin depth, assuming a constant thermal inertia throughout the mission of 300 J m^{-2} K^{-1} s$^{-1/2}$, albedo of 0.2, and emissivity of 0.9. Water vapour diffusion through the regolith is modelled as Fickian following diffusion advection and a temperature-dependent diffusivity. At the surface–atmosphere interface, a mass conservation boundary condition is applied and the surface boundary is set to REMS measurements.

The 2-layer model that it is used to interpret DAN daytime active mode measurements data corresponds to 2 layers with different contents of hydrogen. There are three free parameters of this model: H_2O wt% in the top layer, thickness or cutoff depth where transition between the top and bottom layer takes place, and H_2O wt% in the bottom layer. These three values are obtained by optimization of the retrieval for each particular site that is investigated with active DAN measurements along 9 km of traverse.

Received 5 December 2014; accepted 9 March 2015; published online 13 April 2015

References

1. McKay, C. P. in *Life as we know it* (ed. Seckback, J.) 373–382 (Springer, 2006).
2. McEwen, A. S. *et al.* Recurring slope lineae in equatorial regions of Mars. *Nature Geosci.* **7,** 53–58 (2013).
3. Leshin, L. *et al.* Volatile, isotope and organic analysis of martian fines with the Mars Curiosity Rover. *Science* **341,** 6153 (2013).
4. Ming, D. W. *et al.* Volatile and organic compositions of sedimentary rocks in Yellowknife Bay, Gale crater, Mars. *Science* **343,** 6169 (2014).
5. Möhlmann, D. & Thomsen, K. Properties of cryobrines on Mars. *Icarus* **212,** 123–130 (2011).
6. Nuding, D. L. *et al.* Deliquescence and efflorescence of calcium perchlorate: An investigation of stable aqueous solutions relevant to Mars. *Icarus* **243,** 420–428 (2014).
7. Zorzano, M-P., Mateo-Martí, E., Prieto-Ballesteros, O., Osuna, S. & Renno, N. Stability of liquid saline water on present day Mars. *Geophys. Res. Lett.* **36,** L20201 (2009).
8. Rummel, J. D. A new analysis of Mars 'Special Regions': Findings of the second MEPAG Special Regions Science Analysis Group (SR-SAG2). *Astrobiology* **14,** 887–968 (2014).
9. Archer, P. D. Jr *et al.* in *44th Lunar Planet. Sci. Conf.* 2168 (Lunal and Planetary Institute, 2013).
10. Leighton, R. B. & Murray, B. C. Behavior of carbon dioxide and other volatiles on Mars. *Science* **153,** 136–144 (1966).
11. Martínez, G. M. & Renno, N. Water and brines on Mars: Current evidence and implications for MSL. *Space Sci. Rev.* **175,** 29–51 (2013).
12. Möhlmann, D. Latitudinal distribution of temporary liquid cryobrines on Mars. *Icarus* **214,** 236–239 (2011).
13. Smith, M. D. Interannual variability in TES atmospheric observations of Mars during 1999–2003. *Icarus* **167,** 148–165 (2004).
14. Gomez-Elvira, J. *et al.* REMS: An environmental sensor suite for the Mars science laboratory. *Space Sci. Rev.* **170,** 583–640 (2012).
15. Grotzinger, J. P. *et al.* Mars science laboratory mission and science investigation. *Space Sci. Rev.* **170,** 5–56 (2012).
16. Kereszturi, A. & Rivera-Valentin, E. G. Locations of thin liquid water layers on present-day Mars. *Icarus* **221,** 289–295 (2012).
17. Hudson, T. L., Zent, A., Hecht, M. H., Wood, S. & Cobos, D. in *40th Lunar Planet. Sci. Conf.* 1804–1805 (Lunal and Planetary Institute, 2009).
18. Zent, A. P. *et al.* Initial results from the thermal and electrical conductivity probe (TECP) on Phoenix. *J. Geophys. Res.* **115,** E00E14 (2010).
19. Harri, A-M. *et al.* Mars science laboratory relative humidity observations: Initial results. *J. Geophys. Res.* **119,** 2132–2147 (2014).
20. Richardson, M. I., Toigo, A. D. & Newman, C. E. PlanetWRF: A general purpose, local to global numerical model for planetary atmospheric and climate dynamics. *J. Geophys. Res.* **112,** E09001 (2007).
21. Litvak, M. L. *et al.* The Dynamic Albedo of Neutrons (DAN) experiment NASA's 2009 Mars Science Laboratory. *Astrobiology* **8,** 605–612 (2008).
22. Mitrofanov, I. G. *et al.* in *45th Lunar Planet. Sci. Conf.* 1436 (Lunal and Planetary Institute, 2014).
23. Meslin, P-Y. *et al.* Soil diversity and hydration as observed by ChemCam at Gale Crater, Mars. *Science* **341,** 6153 (2013).
24. Wang, A., Feldman, W. C., Mellon, M. T. & Zheng, M. The preservation of subsurface sulfates with mid-to-high degree of hydration in equatorial regions on Mars. *Icarus* **226,** 980–991 (2013).
25. Keller, J. M. *et al.* Equatorial and midlatitude distribution of chlorine measured by Mars Odyssey GRS. *J. Geophys. Res.* **111,** E03S08 (2006).

© 2015 Macmillan Publishers Limited. All rights reserved

26. Arvidson, R. E. *et al.* Spirit Mars Rover Mission: Overview and selected results from the northern Home Plate Winter Haven to the side of Scamander crater. *J. Geophys. Res.* **115,** E00F03 (2010).
27. Sqyres, S. W. *et al.* Exploration of Victoria Crater by the Mars Rover Opportunity. *Science* **324,** 1058–1061 (2009).
28. Ojha, L. *et al.* Spectral constraints on the formation mechanism of recurring slope lineae. *Geophys. Res. Lett.* **40,** 5621–5626 (2013).
29. Navarro-González, R. *et al.* in *45th Lunar Planet. Sci. Conf.* 2909 (Lunal and Planetary Institute, 2014).
30. Vargel, C. J. & Schmidt, M. P. *Corrosion of Aluminium* (Elsevier B. V., 2004).

Acknowledgements

We are grateful to all of the scientists and engineers who spent many years working to make the MSL mission such a success. We also acknowledge the contribution of the COSPAR Special Region Panel, and J-F. Buenestado-Castro for his support in the documentation process. Part of the research was carried out at the Jet Propulsion Laboratory, California Institute of Technology, under a contract with the National Aeronautics and Space Administration.

Author contributions

F.J.M-T. and M-P.Z. designed the study, prepared the figures, and led the writing of the paper with contributions from the rest of the authors. P.V-S. processed REMS data. A-M.H., M.G. and O.K. processed RHS/REMS data. E.G.R-V. and V.F.C. provided subsurface model simulations. I.J. and C.H. processed DAN data. A.S.M. provided RSL images. All the authors contributed to the analysis discussion, and to the writing process.

Additional information

Supplementary information is available in the online version of the paper. Reprints and permissions information is available online at www.nature.com/reprints. Correspondence and requests for materials should be addressed to F.J.M-T.

Competing financial interests

The authors declare no competing financial interests.

[1]Instituto Andaluz de Ciencias de la Tierra (CSIC-UGR), 18100 Armilla, Granada, Spain. [2]Division of Space Technology, Department of Computer Science, Electrical and Space Engineering, Luleå University of Technology, S98192 Kiruna, Sweden. [3]Centro de Astrobiología (INTA-CSIC), 28850 Torrejón de Ardoz, Madrid, Spain. [4]Earth Observation Research, Finnish Meteorological Institute, 00101 Helsinki, Finland. [5]Arecibo Observatory, Universities Space Research Association, Arecibo, Puerto Rico 00612, USA. [6]Jet Propulsion Laboratory, California Institute of Technology, Pasadena, California 91109, USA. [7]School of Earth and Atmospheric Sciences, Georgia Institute of Technology, Atlanta, Georgia 30332, USA. [8]Niels Bohr Institute, University of Copenhagen, Øster Voldgade 5-7, DK-1350 Copenhagen, Denmark. [9]Max-Planck-Institut für Sonnensystemforschung, Justus-von-Liebig-Weg 3, D-37077 Göttingen, Germany. [10]Lunar and Planetary Lab, University of Arizona, Tucson, Arizona 210063, USA. [11]Arizona State University, Tempe, Arizona 85281, USA. [12]College of Engineering University of Michigan, Ann Arbor, Michigan 48109, USA. [13]Arkansas Center for Space and Planetary Sciences, University of Arkansas, Fayetteville, Arkansas 72701, USA. [14]Laboratorio de Química de Plasmas y Estudios Planetarios, Instituto de Ciencias Nucleares, Universidad Nacional Autónoma de México, Mexico D.F. 04510, México. [15]Instituto de Geociencias (CSIC-UCM), 28040 Madrid, Spain. [16]NASA Goddard Space Flight Center, Greenbelt, Maryland 20771, USA. [17]Department of Astronomy, University of Maryland, College Park, Maryland 20742, USA. [18]UK Centre for Astrobiology, School of Physics and Astronomy, Edinburgh EH9 3JZ, UK. [19]IRAP, Université Toulouse, CNRS, 14 avenue Edouard Belin, 31400 Toulouse, France. [20]Department of Earth and Planetary Sciences, University of California, Davis, California 95616, USA. [21]Planetary Science Institute, Tucson, Arizona 85719, USA. *e-mail: javier.martin-torres@ltu.se

© 2015 Macmillan Publishers Limited. All rights reserved